3. Current distribution in superconducting domains interacting with magnetizable bodies and voltage-driven normal conducting coils – The coupled equivalent electric and magnetic networks

Introduction

In this chapter the models of the equivalent electric and magnetic networks, developed in chapter 1 and 2 respectively, are coupled together to study the problem of a superconducting bulk interacting with a magnetizable body and a voltage-driven normal conducting coil. Through this configuration large number of superconducting devices can be schematized. The electric and the magnetic networks allow to calculate respectively the distribution of current density inside the superconductor and magnetization inside the magnetizable body; these two distributions are not independent, therefore the two networks result coupled. Moreover, since the current of the normal conducting coil is not an assigned quantity, both the networks are coupled with the circuit which drives the coil.

In section 3.1 the mathematical formulation of the field problem is stated. In section 3.2 the discretization technique yet developed in sections 1.2 and 2.2 is applied and the coupling between the electric and the magnetic network is discussed. In section 3.3 an expression of the voltage across the coil, as a function of the current of the superconductor and the magnetization of the magnetizable body is found. This relation allow the coupling of the two networks with the circuit which drives the coil. In section 3.4 an equivalent circuit of a magnetic shield type SFCL is derived by means of the model and compared with standard equivalent circuits available in technical literature.

3.1 The mathematical formulation

Let us consider a system made of a superconducting (SC) domain placed in the vicinity of a magnetizable (M) region and subject to the magnetic field produced by currents flowing in normal conducting (NC) region driven by a time varying voltage generator. We assume that the *quasistatic* approximation holds, i.e. the unique source (the voltage generator) changes on characteristic time scales which are low enough compared with the time required by an electromagnetic wave to propagate over the entire extension of the system. We model the behavior of the superconductor by means of the induced shielding currents **J**, i.e. we assume that no magnetization is induced inside. The normal conducting region is also supposed to have a current distribution $\mathbf{J}^{ext}$ and zero magnetization. For what concern the magnetizable region we assume that an induced magnetization **M** can exists and no currents circulate inside. The electric field **E** at any point of the SC region is related to the local current density **J** by means of the constitutive relation of the superconducting material. Similarly, the magnetization **M** at any point of the M region is related to the local magnetic flux density **B** by means of the constitutive relation of the magnetizable material.

In section 1.2 we have seen as, following the $\mathbf{A}-\varphi$ formulation of *magnetoquasistatics*, the electric field at any point of the space can be expressed through the sum of the gradient of an electric scalar potential φ and the time derivative of the magnetic vector potential **A**, both with the negative sign (equation 1.2.9). Moreover, in section 2.1 we have seen that the magnetic vector potential **A** produced at any point by a distribution of currents and magnetization can be expressed as follows

$$\mathbf{A}(\mathbf{x},t)=\frac{\mu_0}{4\pi}\int_{V_\infty}\frac{\mathbf{J}(\mathbf{x}',t)}{|\mathbf{x}-\mathbf{x}'|}d^3\mathbf{x}'+\frac{\mu_0}{4\pi}\int_{V_\infty}\frac{\mathbf{M}(\mathbf{x}',t)\times(\mathbf{x}-\mathbf{x}')}{|\mathbf{x}-\mathbf{x}'|^3}d^3\mathbf{x}' \qquad (3.1.1)$$

It follows that the magnetic vector potential and the electric field at any point of the considered system are expressed respectively as

$$\mathbf{A}(\mathbf{x},t)=\frac{\mu_0}{4\pi}\int_{V_{NC}}\frac{\mathbf{J}^{ext}(\mathbf{x}',t)}{|\mathbf{x}-\mathbf{x}'|}d^3\mathbf{x}'+ \\ +\frac{\mu_0}{4\pi}\int_{V_{SC}}\frac{\mathbf{J}(\mathbf{x}',t)}{|\mathbf{x}-\mathbf{x}'|}d^3\mathbf{x}'+\frac{\mu_0}{4\pi}\int_{V_M}\frac{\mathbf{M}(\mathbf{x}',t)\times(\mathbf{x}-\mathbf{x}')}{|\mathbf{x}-\mathbf{x}'|^3}d^3\mathbf{x}' \tag{3.1.2}$$

and

$$\mathbf{E}(\mathbf{x},t)=-\nabla\varphi(\mathbf{x},t)-\frac{\mu_0}{4\pi}\frac{\partial}{\partial t}\int_{V_{NC}}\frac{\mathbf{J}^{ext}(\mathbf{x}',t)}{|\mathbf{x}-\mathbf{x}'|}d^3\mathbf{x}'+ \\ -\frac{\mu_0}{4\pi}\frac{\partial}{\partial t}\int_{V_{SC}}\frac{\mathbf{J}(\mathbf{x}',t)}{|\mathbf{x}-\mathbf{x}'|}d^3\mathbf{x}'-\frac{\mu_0}{4\pi}\frac{\partial}{\partial t}\int_{V_M}\frac{\mathbf{M}(\mathbf{x}',t)\times(\mathbf{x}-\mathbf{x}')}{|\mathbf{x}-\mathbf{x}'|^3}d^3\mathbf{x}' \tag{3.1.3}$$

Moreover, in section 2.1 we have seen as, by applying the Clebsh decomposition, the magnetic field **H** at any point of the space can be split in two components, one related to the currents and one related to the magnetization. The first component is expressed by means of the Biot and Savart law and the second as the gradient of a magnetic scalar potential ψ. If follows that the magnetic field at any point of the considered system can be expressed as

$$\frac{\mathbf{B}(\mathbf{x},t)}{\mu_0}-\mathbf{M}(\mathbf{x},t)= \\ \frac{1}{4\pi}\int_{V_{NC}}\frac{\mathbf{J}^{ext}(\mathbf{x}',t)\times(\mathbf{x}-\mathbf{x}')}{|\mathbf{x}-\mathbf{x}'|^3}d^3\mathbf{x}'+\frac{1}{4\pi}\int_{V_{SC}}\frac{\mathbf{J}(\mathbf{x}',t)\times(\mathbf{x}-\mathbf{x}')}{|\mathbf{x}-\mathbf{x}'|^3}d^3\mathbf{x}'-\nabla\psi(\mathbf{x},t) \tag{3.1.4}$$

where the relation (2.1.1) has been used. Equations (3.1.2) – (3.1.4), together with the property of solenoidality of vectors **J** and **B** and the constitutive relations of the superconducting and the magnetizable materials, form the basis of the model of the coupled equivalent electric and magnetic networks which is discussed in section 3.2.

3.2 The discretized problem and the equivalent electric and magnetic networks

Let us consider the system of figure 3.2.1, made of a superconducting (SC) and a magnetizable (M) domain which do not intersect and subject to the magnetic field produced by the currents flowing in a normal conducting coil (NC) driven by a voltage generator. The dimensions of the SC, M and NC domains and the frequency of variation of external magnetic field are such that the magnetoquasistatic approximation holds.

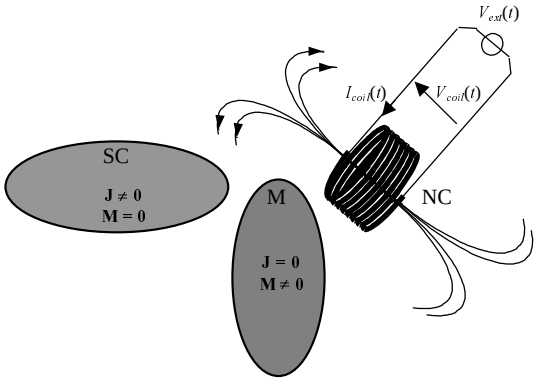

Figure 3.1.1: scheme of the considered system

The electric field **E** at any point of the SC region is related to the local current density **J** by means of the constitutive relation of the superconducting material, that for homogeneous and time invariant superconductors can generically be expressed as

$$\mathbf{E}(\mathbf{x},t) = \mathbf{F}(\mathbf{J}(\mathbf{x},t)) \tag{3.2.1}$$

Similarly, the magnetization **M** at any point of the M region is related to the local magnetic flux density **B** by means of the constitutive relation of the magnetizable material that in the most general case is non linear and hysteretic, and for homogeneous and time invariant materials can be expressed as

$$\mathbf{M}(\mathbf{x},t)=\mathcal{M}_B\left(\mathbf{B}(\mathbf{x},\tau),\tau\le t\right) \tag{3.2.2}$$

Actually both the two constitutive relations depend also on the temperature; in the following we will assume the superconducting region as well as the magnetizable one to be in thermal equilibrium with assigned temperature, thus neglecting the effects of the local heating. For the cases where the thermal effects become important, particularly for the superconductor, the present electromagnetic model must be coupled with a thermal model which allow to calculate at any time, the temperature distribution inside the entire domains. Moreover the electric field of the superconductor depends also on the local magnetic flux density, but we do not indicate explicitly this dependence.

In order to determine the distribution of current density inside the superconductor let us divide the superconducting and the magnetizable region in a finite number $N_{E|SC}$ and $N_{E|M}$ of three-dimensional elements, respectively. Let $N_{F|SC}$ be the total number of faces of the discretized SC region and let $N_{C|SC}$ be the number of faces through which a current flows; any of these faces is shared by two elements. The remaining ($N_{F|SC} - N_{C|SC}$) faces lie on the boundary of the SC domain and do not carry any current. Concerning the magnetizable region, let $N_{F|M}$ be the total number of faces; $N_{F|MB}$ of these faces lie on the boundary of the SC body while $N_{F|MI}$ are inner faces. Let us also define a normal unit vector for all faces both of the SC and of the M region. We assume the following quantities as unknowns of the problem:

- the set **I**(t) of the $N_{C|SC}$ currents flowing through all the faces of the discretized SC region which do not lie on the boundary
- the set **V**(t) of the $N_{E|SC} - 1$ electric scalar potentials of the centers of all the elements of the discretized SC region less one to whom we assign value zero (reference node)
- the set Φ(t) of the $N_{F|M}$ magnetic fluxes through the faces of the discretized M region

- the set Ψ(t) of the $N_{E|M} - 1$ magnetic scalar potentials in the centers of all the elements of the discretized M region less one to whom we assign value zero (reference node)

The current and the fluxes are assumed to be oriented according to the normal unit vector of the corresponding face. In order to expressed all the physical quantities involved in the calculation as a function of unknowns of the problem we assume the current density to be an uniform vector inside any element of the SC domain. Its value can be related to the currents through the faces of the discretization by means of the procedure of minimum error described in section 2.1, i.e.

$$\mathbf{J}(\mathbf{x},t) = [\mathbf{K}_J(\mathbf{x})]\mathbf{I}(t) \tag{3.2.3}$$

Similarly we assume the magnetic flux density to be an uniform vector inside any element of the M domain an express it as a function of the fluxes through the faces of the discretization as follows

$$\mathbf{B}(\mathbf{x},t) = [\mathbf{K}_B(\mathbf{x})]\mathbf{\Phi}(t) \tag{3.2.4}$$

The details of the procedure of minimum error and the properties of matrixes $[\mathbf{K}_J(\mathbf{x})]$ and $[\mathbf{K}_B(\mathbf{x})]$ are all listed at pages 18-20 and 74. Moreover, for what concern the current density of the normal conducting coil we assume that it distributes uniformly inside any turn and we express it as

$$\mathbf{J}^{ext}(\mathbf{x},t) = \mathbf{k}_{NC}(\mathbf{x})I_{coil}(t) \tag{3.2.5}$$

where $\mathbf{k}_{NC}(\mathbf{x})$ is the vector given by the ratio between the unit vector tangent to the direction of the turn at point **x** and the area of its cross section and oriented in a way to be outgoing from the positive terminal of the coil and ingoing to the negative one.

Let us associate, according to the procedures described in sections 1.2 and 2.2 (see pages 11 and 71) two graphs $\mathcal{G}_{SC}$ and $\mathcal{G}_M$ to the meshes of the superconducting and

magnetizable region respectively. Concerning the graph $\mathcal{G}_{SC}$ we notice that the two additional nodes representing the electrode of the generator do not need to be introduced in the present case, for no transport current is considered in the superconductor.

The solenoidality of vector **J** requires that all the currents flowing through the faces of any element of the SC mesh have zero algebraic sum. The $N_{E|SC} - 1$ independent equation of these type for the $N_{C|SC}$ currents of the superconducting region can be easily expressed through the incidence matrix of graph $\mathcal{G}_{SC}$, as follows

$$[\mathbf{A}_{SC}]\mathbf{I}(t) = \mathbf{0} \tag{3.2.6}$$

where the $(N_{E|SC} - 1) \times N_{C|SC}$ matrix $[\mathbf{A}_{SC}]$ is extracted from the incidence matrix of graph $\mathcal{G}_{SC}$, by suppressing the row referring to a node chosen as the reference one.

Similarly, the solenoidality of vector **B** imposes to all fluxes through the faces of any element of the M mesh to have zero algebraic sum. $N_{E|M} - 1$ independent equation of these type for the $N_{F|M}$ fluxes of the magnetizable region can be expressed through the incidence matrix of graph $\mathcal{G}_{M}$, as follows

$$[\mathbf{A}_{M}]\mathbf{\Phi}(t) = \mathbf{0} \tag{3.2.7}$$

where the $(N_{E|M} - 1) \times N_{F|M}$ matrix $[\mathbf{A}_{M}]$ is extracted from the incidence matrix of graph $\mathcal{G}_{M}$, by suppressing the rows referring to a node chosen as the reference one and to node ∞.

Let us now consider equation (3.1.4) applied to a point **x** lying inside the magnetizable region. This equation relates the total magnetic field to the currents of the superconductor and the coil and the magnetic scalar potential. By taking the line integral of the magnetic field over a path connecting whatever couple of points $\mathbf{x}_h$ and $\mathbf{x}_k$ belonging to the M domain and oriented from $\mathbf{x}_h$ to $\mathbf{x}_k$ the following equation is obtained:

$$\int_{\mathbf{x}_h}^{\mathbf{x}_k} \frac{\mathbf{B}(\mathbf{x},t)}{\mu_0}\cdot d\mathbf{x} - \int_{\mathbf{x}_h}^{\mathbf{x}_k} \mathbf{M}(\mathbf{x},t)\cdot d\mathbf{x} = \psi(\mathbf{x}_h,t) - \psi(\mathbf{x}_k,t) + \\ + \int_{\mathbf{x}_h}^{\mathbf{x}_k}\left(\frac{1}{4\pi}\int_{V_{NC}} \frac{\mathbf{J}^{ext}(\mathbf{x}',t)\times(\mathbf{x}-\mathbf{x}')}{|\mathbf{x}-\mathbf{x}'|^3} d^3\mathbf{x}'\right)\cdot d\mathbf{x} + \int_{\mathbf{x}_h}^{\mathbf{x}_k}\left(\frac{1}{4\pi}\int_{V_{SC}} \frac{\mathbf{J}(\mathbf{x}',t)\times(\mathbf{x}-\mathbf{x}')}{|\mathbf{x}-\mathbf{x}'|^3} d^3\mathbf{x}'\right)\cdot d\mathbf{x} \tag{3.2.8}$$

All the terms of this equation have the dimensions of a magneto-motive force. By considering the mesh of the magnetizable domain, it is possible to associate at any face that does not lie on the boundary an equation of the same type of (3.2.8). In fact, to any of the $N_{F|MI}$ inner faces it corresponds an integration path made of the union of the segments connecting the centre of the face to the centers of the elements which share it; this integration path is oriented according to the normal unit vector of the face. By substituting equations (3.2.3) - (3.2.5) in equation (3.2.8) and considering the constitutive relation (3.2.2) we obtain

$$\left(\int_{\mathbf{x}_h}^{\mathbf{x}_k} \frac{d\mathbf{x}^T[\mathbf{K}_B(\mathbf{x})]}{\mu_0}\right)\boldsymbol{\Phi}(t) - \int_{\mathbf{x}_h}^{\mathbf{x}_k} d\mathbf{x}^T \mathcal{M}_B([\mathbf{K}_B(\mathbf{x})]\boldsymbol{\Phi}(\tau),\tau\le t) = \\ \psi(\mathbf{x}_h,t) - \psi(\mathbf{x}_k,t) + I_{coil}(t)\int_{\mathbf{x}_h}^{\mathbf{x}_k} d\mathbf{x}^T\left(\frac{1}{4\pi}\int_{V_{NC}} \frac{\mathbf{k}_{NC}(\mathbf{x}')\times(\mathbf{x}-\mathbf{x}')}{|\mathbf{x}-\mathbf{x}'|^3} d^3\mathbf{x}'\right) + \\ + \int_{\mathbf{x}_h}^{\mathbf{x}_k} d\mathbf{x}^T\left(\frac{1}{4\pi}\int_{V_{SC}} \frac{[\mathbf{K}_J(\mathbf{x}')]\mathbf{I}(t)\times(\mathbf{x}-\mathbf{x}')}{|\mathbf{x}-\mathbf{x}'|^3} d^3\mathbf{x}'\right) \tag{3.2.9}$$

The line integral from $\mathbf{x}_h$ to $\mathbf{x}_k$ can be split in the sum of the integrals from $\mathbf{x}_h$ to the centre of the face shared by the two elements and from the latter to $\mathbf{x}_k$. Since matrix $[\mathbf{K}_B(\mathbf{x})]$ is element wise uniform, the integrating function $\mathcal{M}_B$ can be moved out and the second integral of the left side can be expressed as the product of a non linear function of the fluxes with a vector of geometrical coefficients. However, if the considered material is not homogeneous, the constitutive relation depends explicitly on the point and this manipulation cannot be applied.

Equation (3.2.9) states a link, which in general is non linear and hysteretic, between the fluxes of the M region and the currents of the superconducting region and the

external coil. The link is linear in case of linear magnetizable material. Likewise the case of equation (2.2.8) equation (3.2.9) can be seen as the instantaneous balance of the magneto-motive forces relative to a magnetic circuit branch derived from two nodes *h* and *k* with potential $\psi(\mathbf{x}_h,t)$ and $\psi(\mathbf{x}_k,t)$ respectively and containing a magneto-motive force generator $m^{ext}{}_i(t)$ related to the current of the coil, a linear flux-controlled magneto-motive force generator $m^{0}{}_i(t)$ and a non linear flux-controlled magneto-motive force generator $m^{M}{}_i(t)$ related to the magnetization and an additional magneto-motive force generator $m^{SC}{}_i(t)$ related to the currents of the SC region. This latter contribute can be expressed as the product of a vector of dimensionless coefficients $\boldsymbol{n}_i^{SC}$ with the vector of the unknown currents $\mathbf{I}(t)$. A picture of the circuit branch is shown in figure 3.2.2.

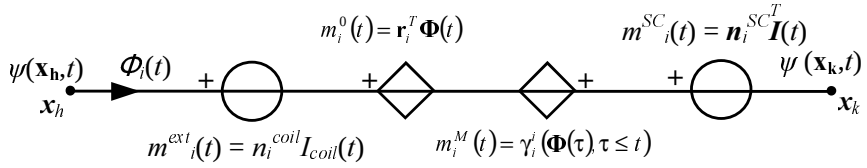

figure 3.2.2: circuit scheme of equation (3.2.9)

By using the symbols introduced in the figure, equation (2.2.7) can be rewritten as

$$\psi(\mathbf{x}_h,t) - \psi(\mathbf{x}_k,t) - \mathbf{n}_i^{SC\,T}\mathbf{I}(t) - n_i^{coil} I_{coil}(t) = \mathbf{r}_i^T \boldsymbol{\Phi}(t) - \gamma_i^i(\boldsymbol{\Phi}(\tau), \tau \le t) \qquad (3.2.10)$$

where *T* denotes the transpose operator. An equation of the type of (3.2.10) can be associated at every of the faces of the M domain which do not lie on the boundary; the set of these $N_{F|MI}$ independent equations can be written concisely as

$$[\mathbf{A}_{M_{RED}}]^T \boldsymbol{\Psi}(t) - [\mathbf{N}^{SC}]\,\mathbf{I}(t) - \mathbf{N}^{coil} I_{coil}(t) = [\mathbf{R}]\boldsymbol{\Phi}(t) + \boldsymbol{\Gamma}_I(\boldsymbol{\Phi}(\tau), \tau \le t) \qquad (3.2.11)$$

Matrix $[\mathbf{A}_{M_{RED}}]$, having dimension $N_{F|MI} \times (N_{E|M} - 1)$, is obtained from matrix $[\mathbf{A}_M]$ of equation (3.2.7) by eliminating the columns referring to the fluxes associated to the boundary faces, $[\mathbf{N}^{SC}]$ is the $N_{F|MI} \times N_{C|SC}$ matrix of reluctances obtained by staking

vectors $\boldsymbol{n}_i^{SC}$ of all equations (3.2.10), $\mathbf{N}^{coil}$ is the vector of the $N_{F|MI}$ coefficients n_i^{coil}, **[R]** is the $N_{F|MI} \times N_{F|M}$ matrix of reluctances obtained by staking vectors $\mathbf{r}_i^T$ of all equations (3.2.10) and $\boldsymbol{\Gamma}_I(\boldsymbol{\Phi}(\tau), \tau \le t)$ is the vector of the $N_{F|MI}$ scalar function $\gamma_i^I(\boldsymbol{\Phi}(\tau), \tau \le t)$. The subscript $_I$ of function Γ denotes that it refers to inner faces.

Matrix equations (3.2.7) and (3.2.11), being ($N_{E|M} - 1 + N_{F|MI}$) scalar equations, do not allow to calculate the potentials of the nodes and the fluxes through the faces when the current of the superconducting and the regions are specified, for the latter are ($N_{E|M} - 1 + N_{F|MI} + N_{F|MB}$) in total and therefore further $N_{F|MB}$ equations must be stated. However, as discussed in section 2.2, these $N_{F|MB}$ missing equations can be specified by relating the fluxes through the boundary faces to the magnetization M region and to the currents of the SC and NC regions. According to the stokes theorem the magnetic flux through a generic surface can be expressed by means of the loop integral over the border of the face of the vector magnetic potential, which is given by equation 3.1.2; therefore the magnetic flux $\Phi_j(t)$ at time t through the generic face j lying on the boundary of the magnetizable region can be expressed as

$$\Phi_j(t) = \oint_{\partial\Sigma_j} \left(\frac{\mu_0}{4\pi} \int_{V_{NC}} \frac{\mathbf{J}^{ext}(\mathbf{x}', t)}{|\mathbf{x} - \mathbf{x}'|} d^3\mathbf{x}' \right) \cdot d\mathbf{x} + \oint_{\partial\Sigma_j} \left(\frac{\mu_0}{4\pi} \int_{V_{SC}} \frac{\mathbf{J}(\mathbf{x}', t)}{|\mathbf{x} - \mathbf{x}'|} d^3\mathbf{x}' \right) \cdot d\mathbf{x} + \oint_{\partial\Sigma_j} \left(\frac{\mu_0}{4\pi} \int_{V_{SC}} \frac{\mathbf{M}(\mathbf{x}', t) \times (\mathbf{x} - \mathbf{x}')}{|\mathbf{x} - \mathbf{x}'|^3} d^3\mathbf{x}' \right) \cdot d\mathbf{x} \tag{3.2.12}$$

where $\partial\Sigma_j$ represents the border line of face j. By substituting and the constitutive relation of the magnetizable material (3.2.2) and equations (3.2.3) – (3.2.5) in equation (3.2.12) it follows

$$\begin{aligned}\Phi_j(t) = I_{coil}(t)\oint_{\partial\Sigma_j} d\mathbf{x}^T\left(\frac{\mu_0}{4\pi}\int_{V_{NC}}\frac{\mathbf{k}_{NC}(\mathbf{x}')}{|\mathbf{x}-\mathbf{x}'|}d^3\mathbf{x}'\right)+\\ +\left[\oint_{\partial\Sigma_j} d\mathbf{x}^T\left(\frac{\mu_0}{4\pi}\int_{V_{SC}}\frac{[\mathbf{K}_J(\mathbf{x}')]}{|\mathbf{x}-\mathbf{x}'|}d^3\mathbf{x}'\right)\right]\mathbf{I}(t)+\\ +\oint_{\partial\Sigma_j}\left(\frac{\mu_0}{4\pi}\int_{V_{SC}}\frac{\mathcal{M}_B([\mathbf{K}_B(\mathbf{x}')]\boldsymbol{\Phi}(\tau),\tau\le t)\times(\mathbf{x}-\mathbf{x}')}{|\mathbf{x}-\mathbf{x}'|^3}d^3\mathbf{x}'\right)\cdot d\mathbf{x}\end{aligned} \tag{3.2.13}$$

The above equation allows to see the flux through face *j* lying on the boundary as composed by three contributes: a first contribute $\Phi_j^{coil}(t)$, proportional to the current of the normal coil through a coefficient l_j^{coil} having the dimension of an inductance, a second contribute $\Phi_j^{SC}(t)$, given by the product of a vector $\mathbf{l}_j^{sc}$ of coefficients with the dimension of an inductance and the vector **I**(*t*) of the currents flowing through the faces of the SC region, and a third contribute $\Phi_j^{m}(t)$ related to the magnetization of the superconductor, and expressed (in general) by a non linear and hysteretic function of all fluxes $\gamma_j^b(\boldsymbol{\Phi}(\tau),\tau\le t)$, i. e.

$$\Phi_j(t) = l_j^{coil} I_{ext}(t) + \mathbf{l}_j^{SC}\mathbf{I}(t) + \gamma_j^b(\boldsymbol{\Phi}(\tau),\tau\le t) \tag{3.2.14}$$

Maintaining the circuit view of the problem we can see the flux through the boundary face *j*, to whom correspond a branch of the graph which converges to node ∞, as produced by two independent and a controlled flux generator, as shown in figure 3.2.3.

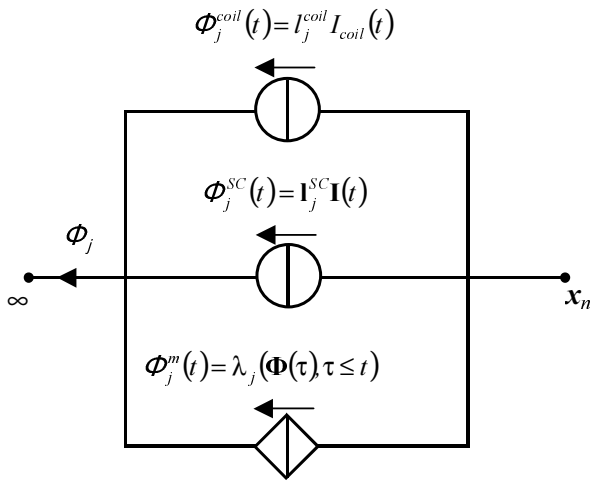

figure 3.2.3: circuit scheme of equation (2.2.14)

The node $\boldsymbol{x}_n$ coincides with the center of the element to which the boundary face *j* belongs to, while the node ∞ represents the far surface (placed at infinity) where all the lines of the magnetic flux density shut up, as discussed in section 2.2 (see pages 80-81).

The set of the $N_{F|MB}$ independent equations of the type of the (3.2.14), which express the fluxes through the boundary faces as a function of all the fluxes and the currents of the superconducting and the normal regions, can be written in the following way

$$[\mathbf{S}]\boldsymbol{\Phi}(t) = \mathbf{L}^{coil}\, I_{coil}(t) + \left[\mathbf{L}^{SC}\right] \mathbf{I}(t) + \Gamma_B(\boldsymbol{\Phi}(\tau), \tau \le t) \qquad (3.2.15)$$

where **[S]** is a matrix having dimension $N_{F|MB} \times N_{F|M}$, whose generic element s_{ij} is equal to 1 if the *j-th* flux of vector $\boldsymbol{\Phi}(t)$ flows through the *i-th* boundary face and is equal to 0 otherwise, $\mathbf{L}^{coil}$ is the vector of the $N_{F|MB}$ coefficients l_j^{coil} of equation (3.2.14), $\left[\mathbf{L}^{SC}\right]$ is the $N_{F|MB} \times N_{C|SC}$ matrix of inductances obtained by staking vectors $\mathbf{l}_j^{SC}$ of equation (3.2.15), and $\boldsymbol{\Gamma}_B(\boldsymbol{\Phi}(\tau), \tau \le t)$ is the vector of the N_{FB} scalar function $\gamma_j^b(\boldsymbol{\Phi}(\tau), \tau \le t)$. The subscript $_B$ of function Γ denotes that it refers to boundary faces.

From equations (3.2.7), (3.2.11) and (3.2.15) it follows that the entire magnetizable domain can be schematized by means of an equivalent magnetic network, having $N_{F|M}$

branches and ($N_{E|M} + 1$) nodes. The circuit unknowns are $N_{F|M}$ fluxes through the faces and ($N_{E|M} - 1$) potentials of the nodes (the potential of the reference node is arbitrarily assumed to be equal to zero and the potential of node ∞ cannot be determined). This equivalent magnetic network, which allows to calculate the magnetization distribution inside the M region, contains forcing components (magneto-motive force and magnetic fluxes generators) which depend on the currents of the superconductor and the coil. An elemental cell of the magnetic circuit associated to an element of the mesh having the face Σ_{ABCD} lying on the boundary of magnetizable domain is shown in figure 3.2.4, which is the assembling of figure 3.2.2 and 3.2.3. The linear and the non linear reluctances represent the linear and the non linear flux-controlled magneto-motive force generators of figure 3.2.2. Even though less rigorous, this latter representation coincides with the former one if we agree that the reluctances "feel" the fluxes of all the branches connected to the center of the considered element.

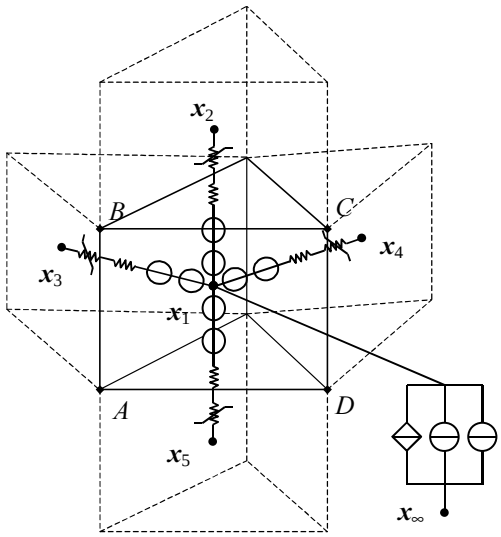

figure 3.2.4:elemental cell of the equivalent magnetic circuit associated to an element with a face lying on the boundary

The solving system of the equivalent magnetic network, that is a set of ($N_{F|M} + N_{E|M} - 1$) equations relating the ($N_{F|M} + N_{E|M} - 1$) unknowns can be written as

$$\begin{cases} [\mathbf{A}_M]\boldsymbol{\Phi}(t) = \mathbf{0} \\ [\mathbf{A}_{M_{RED}}]^T \boldsymbol{\Psi}(t) - [\mathbf{N}^{SC}]\mathbf{I}(t) - \mathbf{N}^{coil} I_{coil}(t) = [\mathbf{R}]\boldsymbol{\Phi}(t) + \boldsymbol{\Gamma}_I(\boldsymbol{\Phi}(\tau), \tau \le t) \\ [\mathbf{S}]\boldsymbol{\Phi}(t) = \mathbf{L}^{coil} I_{coil}(t) + [\mathbf{L}^{SC}]\mathbf{I}(t) + \Gamma_B(\boldsymbol{\Phi}(\tau), \tau \le t) \end{cases} \quad (3.2.16)$$

The vectors of the unknown fluxes and potentials cannot be calculated since system (3.2.16) contains forcing terms that depend on the currents $\mathbf{I}(t)$ through the faces of the superconducting domain and the current $I_{coil}(t)$ circulating in the coil, which are not known quantities. In order to specify the vector $\mathbf{I}(t)$ let us now consider equation (3.1.3) applied to a point $\mathbf{x}$ lying inside the superconducting region. This equation relates the electric field to the electric scalar potential, the currents of the superconductor and the coil and the magnetization of the M region. By taking the line integral of the electric field over a path connecting whatever couple of points $\mathbf{x}_h$ and $\mathbf{x}_k$ belonging to the SC domain and oriented from $\mathbf{x}_h$ to $\mathbf{x}_k$ the following equation is obtained:

$$\begin{aligned} \int_{\mathbf{x}_h}^{\mathbf{x}_k} \mathbf{E}(\mathbf{x},t)\cdot d\mathbf{x} &= \varphi(\mathbf{x}_h,t) - \varphi(\mathbf{x}_k,t) - \frac{d}{dt}\int_{\mathbf{x}_h}^{\mathbf{x}_k}\left(\frac{\mu_0}{4\pi}\int_{V_{NC}}\frac{\mathbf{J}^{ext}(\mathbf{x}',t)}{|\mathbf{x}-\mathbf{x}'|}d^3\mathbf{x}'\right)\cdot d\mathbf{x} + \\ &- \frac{d}{dt}\int_{\mathbf{x}_h}^{\mathbf{x}_k}\left(\frac{\mu_0}{4\pi}\int_{V_{SC}}\frac{\mathbf{J}(\mathbf{x}',t)}{|\mathbf{x}-\mathbf{x}'|}d^3\mathbf{x}'\right)\cdot d\mathbf{x} - \frac{d}{dt}\int_{\mathbf{x}_h}^{\mathbf{x}_k}\left(\frac{\mu_0}{4\pi}\int_{V_M}\frac{\mathbf{M}(\mathbf{x}',t)\times(\mathbf{x}-\mathbf{x}')}{|\mathbf{x}-\mathbf{x}'|^3}d^3\mathbf{x}'\right)\cdot d\mathbf{x} \end{aligned} \quad (3.2.17)$$

All the terms of this equation have the dimension of a voltage. By considering the mesh of the superconducting domain, it is possible to associate at any face that does not lie on the boundary an equation of the same type of (3.2.17). In fact, to any of the $N_{C|SC}$ inner faces it corresponds an integration path made of the union of the segments connecting the centre of the face to the centers of the elements which share it; this integration path is oriented according to the normal unit vector of the face. By substituting equations (3.2.3) - (3.2.5) and the constitutive relations (3.2.1) and (3.2.2) in equation (3.2.17) and rearranging the terms we obtain

$$\begin{aligned}\varphi(\mathbf{x}_h,t)-\varphi(\mathbf{x}_k,t)=&\int_{\mathbf{x}_h}^{\mathbf{x}_k} d\mathbf{x}^T\mathbf{F}([\mathbf{K}_J(\mathbf{x})]\mathbf{I}(t))\\&+\left(\int_{\mathbf{x}_h}^{\mathbf{x}_k} d\mathbf{x}^T\left(\frac{\mu_0}{4\pi}\int_{V_{NC}}\frac{\mathbf{k}_{NC}(\mathbf{x}')}{|\mathbf{x}-\mathbf{x}'|}d^3\mathbf{x}'\right)\right)\frac{d}{dt}I_{coil}(t)+\\&+\left(\int_{\mathbf{x}_h}^{\mathbf{x}_k} d\mathbf{x}^T\left(\frac{\mu_0}{4\pi}\int_{V_{SC}}\frac{[\mathbf{K}_J(\mathbf{x}')]}{|\mathbf{x}-\mathbf{x}'|}d^3\mathbf{x}'\right)\right)\frac{d}{dt}\mathbf{I}(t)+\\&+\frac{d}{dt}\int_{\mathbf{x}_h}^{\mathbf{x}_k} d\mathbf{x}^T\left(\frac{\mu_0}{4\pi}\int_{V_M}\frac{\mathcal{M}_B([\mathbf{K}_B(\mathbf{x}')]\mathbf{\Phi}(\tau),\tau\le t)\times(\mathbf{x}-\mathbf{x}')}{|\mathbf{x}-\mathbf{x}'|^3}d^3\mathbf{x}'\right)\end{aligned}\tag{3.2.18}$$

By splitting the line integral from $\mathbf{x}_h$ to $\mathbf{x}_k$ in the sum of the integrals over the two segments connecting $\mathbf{x}_h$ to the centre of the face shared by the two elements and the latter to $\mathbf{x}_k$ and considering that both matrix functions $[\mathbf{K}_J(\mathbf{x})]$ and $[\mathbf{K}_B(\mathbf{x})]$ are element wise uniform, it follows that functions **F** and $\mathcal{M}_B$ can be moved out of the relative integrals; the left side term can be then expressed as the product of a vector of geometrical coefficients with a nonlinear function of all currents. Similarly, the last right hand side contribution can be expressed as the product of a vector of geometrical coefficients with the time derivative of a nonlinear function of all fluxes.

Equation (3.2.18) states a link between the currents of the superconducting region, the current of the normal conducting coil and the fluxes of the magnetizable region. Likewise the case of equation (1.2.18) equation (3.2.18) can be seen as the instantaneous balance of the voltage relative to a magnetic circuit branch derived from two nodes *h* and *k* with potential $\varphi(\mathbf{x}_h,t)$ and $\varphi(\mathbf{x}_k,t)$ with respect to the reference node. As discussed in section 1.2 (see pages 22), the first term on the right side represents the local voltage drop associated to the Joule power consumption, while second and the third terms represent the voltage induced by the time change of the magnetic field produced by the current of the coil and the superconductor respectively. The last term takes in account of the voltage induced by the time change of the magnetic field produced by the magnetization of the M region. A picture of the circuit branch is shown in figure 3.2.5.

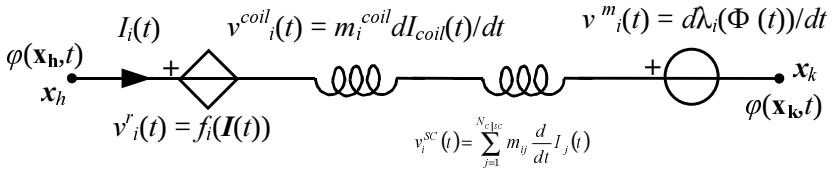

figure 3.2.5: circuit scheme of equation (3.2.18)

By using the symbols introduced in the figure, equation (3.2.18) can be rewritten as

$$\varphi(\mathbf{x}_h,t) - \varphi(\mathbf{x}_k,t) = f_i(\mathbf{I}(t)) + m_i^{coil} \frac{d}{dt} I_{coil}(t) + \sum_{j=1}^{NC} m_{ij} \frac{d}{dt} I_j(t) + \frac{d}{dt} \lambda_i(\mathbf{\Phi}(t)) \quad (3.2.19)$$

An equation of the type of (3.2.19) can be associated at every of the faces of the superconducting domain which can be crossed by a current; the set of these $N_{C|SC}$ independent equations can be written concisely as

$$[\mathbf{A}_{sc}]^T \mathbf{V}(t) = \mathbf{F}(\mathbf{I}(t)) + [\mathbf{M}] \frac{d}{dt} \mathbf{I}(t) + \mathbf{M}^{coil} \frac{d}{dt} I_{coil}(t) + \frac{d}{dt} \mathbf{\Lambda}(\mathbf{\Phi}(\tau), \tau \le t) \quad (3.2.20)$$

where **V**(t) represents the set of the $N_{E|SC} - 1$ electric scalar potentials wtith respect to the reference node. The vector functions $\boldsymbol{F}$ and Λ are obtained by staking the scalar functions f_i and λ_i of any of equation (3.2.20). $\mathbf{M}^{coil}$ is the vector of the $N_{C|SC}$ coefficients m_i^{coil} and **[M]** is the $N_{C|SC} \times N_{C|SC}$ matrix of auto/mutual induction coefficients.

From equations (3.2.6) and (3.2.20) it follows that the entire superconducting domain can be schematized by means of an equivalent electric network, having $N_{C|SC}$ branches and $N_{E|SC}$ nodes. The circuit unknowns are $N_{C|SC}$ fluxes through the faces and ($N_{E|SC} - 1$) potentials of the nodes with respect to the reference one. The solving system of the equivalent electric network, that is a set of ($N_{C|SC} + N_{E|SC} - 1$) independent equations, can be written as

$$\begin{cases} [\mathbf{A}_{SC}]\mathbf{I}(t) = \mathbf{0} \\ [\mathbf{A}_{SC}]^T \mathbf{V}(t) = F(\mathbf{I}(t)) + [\mathbf{M}]\dfrac{d}{dt}\boldsymbol{I}(t) + \mathbf{M}^{coil}\dfrac{d}{dt}I_{coil}(t) + \dfrac{d}{dt}\boldsymbol{\Lambda}(\boldsymbol{\Phi}(\tau), \tau \le t) \end{cases} \tag{3.2.21}$$

The equivalent electric network, that allows to calculate the current distribution inside the SC region, contains components (voltage generators) which depend on the fluxes of equivalent magnetic network. Since also the latter contains forcing components depending on the currents of the equivalent electric network, the two networks result coupled and cannot be solved independently. The coupling is non linear because in general, the constitutive relation of the magnetic material, equation (3.2.2), makes non linear functions Γ_I and Γ_B of system (3.2.16) and function Λ of system (3.2.21). An elemental cell of the electric circuit associated to an element of the mesh having the face Σ_{ABCD} lying on the boundary of superconducting domain is shown in figure 3.2.6. Also in this case the non linear resistance represents the non linear current controlled voltage generators of figure 3.2.5. This representation, which is more physical but less rigorous, coincides with the former one if we agree that the resistance "feels" the currents of all the branches connected to the center of the considered element.

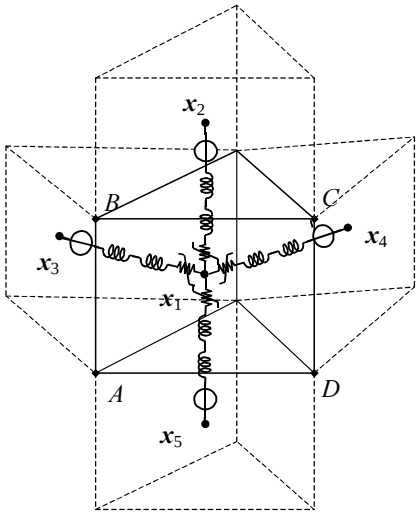

figure 3.2.6: elemental cell of the equivalent electric circuit associated to an element with a face lying on the boundary

If the current $I_{coil}(t)$ flowing in the coil is assigned, systems (3.2.16) and (3.2.20) can be solved together and the unknown vectors $\boldsymbol{I}(t)$, $\Phi(t)$, $\boldsymbol{V}(t)$ and $\Psi(t)$ can be determined. In general this is not the case because the coil is usually voltage rather than current driven and the current $I_{coil}(t)$ is not a known a quantity. Therefore systems (3.2.16) and (3.2.20) contains one unknown more than the equations. However, the voltage $V_{coil}(t)$ across the coil depends on the current of the coil itself, on the shielding currents of the SC region, coil and the SC domain and on the fluxes of the magnetizable region, i.e. in terms of circuit quantities, it depends on $I_{coil}(t)$, $\boldsymbol{I}(t)$ and $\Phi(t)$ and can be generically expressed as

$$V_{coil}(t) = v\left(I_{coil}(\tau), \boldsymbol{I}(\tau), \boldsymbol{\Phi}(\tau), \tau \le t\right) \tag{3.2.22}$$

The specification of this voltage characteristic, i.e. the definition of function v, is the topic of the next section. However, by assuming, for the moment, that function v is provided, and considering that the coil is driven by an external generator which impresses the voltage $V_{ext}(t)$ the following equation can be stated

$$v\left(I_{coil}(\tau), \boldsymbol{I}(\tau), \boldsymbol{\Phi}(\tau), \tau \le t\right) = V_{ext}(t) \tag{3.2.23}$$

Equation (3.2.23) can be coupled with systems (3.2.16) and (3.2.20) to obtain a system containing as many equations as the unknowns which can be solved and the time evolution of the current density at any point of the superconducting domain can be finally reconstructed by means of equation (3.2.3).

If we are not interested in determining the magnetic scalar potentials at the center of the elements of the magnetizable region, it is possible to apply the algebraic procedure described in section 2.2 (see page 83) to eliminate them from system (3.2.16) and obtain a set of $N_{F|M}$ equations relating only the fluxes to the currents. In case of magnetizable region made of linear magnetic material, such a reduced system turns linear and the set of the unknown fluxes can be expressed directly as a function of the currents as follows

$$\mathbf{\Phi}(t) = \left[\mathscr{L}_{SC}\right] \boldsymbol{I}(t) + \ell_{coil} I_{coil}(t) \tag{3.2.24}$$

where $\left[\mathscr{L}_{SC}\right]$ is $N_{F|M} \times N_{C|SC}$ matrix and ℓ_{coil} is a vector of $N_{F|M}$ coefficients. Both the elements of matrix $\left[\mathscr{L}_{SC}\right]$ and vector ℓ_{coil} have the dimension of an inductance. Due to the linearity of the material also function Λ turns linear and system (3.2.21) becomes

$$\begin{cases} [\mathbf{A}_{SC}]\mathbf{I}(t) = \mathbf{0} \\ [\mathbf{A}_{sc}]^T \mathbf{V}(t) = F(\mathbf{I}(t)) + [\mathbf{M}]\dfrac{d}{dt}\boldsymbol{I}(t) + \mathbf{M}^{coil}\dfrac{d}{dt}I_{coil}(t) + [\mathbf{\Lambda}]\dfrac{d}{dt}\mathbf{\Phi}(t) \end{cases} \tag{3.2.25}$$

By substituting equation (3.2.24) in equations (3.2.23) and (3.2.25) it follows

$$\begin{cases} [\mathbf{A}_{SC}]\mathbf{I}(t) = \mathbf{0} \\ [\mathbf{A}_{SC}]^T \mathbf{V}(t) = F(\mathbf{I}(t)) + \\ \qquad + \left([\mathbf{M}] + [\mathbf{\Lambda}]\left[\mathscr{L}_{SC}\right]\right)\dfrac{d}{dt}\boldsymbol{I}(t) + \left(\mathbf{M}^{coil} + [\mathbf{\Lambda}]\ell_{coil}\right)\dfrac{d}{dt}I_{coil}(t) \\ v'\left(I_{coil}(t), \boldsymbol{I}(t)\right) = V_{ext}(t) \end{cases} \tag{3.2.26}$$

where $\boldsymbol{v'}$ denotes function v of equation (3.2.23) after the substitution. As discussed in section 1.3, by applying the tree-cotree decomposition algorithm, system (3.2.26) can be manipulated to obtain one containing only a reduced set of ($N_{C|SC} - N_{E|SC} + 1$) currents plus the current of the coil as unknowns, thus allowing a considerable saving of calculation time and memory requirements; System (3.2.26) is quite suggestive of the fact that matrixes Λ and $\mathscr{L}_{SC}$ and vector ℓ_{coil} take account of the influence of the magnetizable region on the current distribution inside the superconducting one. It is worth to notice that in case of zero magnetization, i.e. in case of no magnetizable domains placed in the vicinity of the superconducting region and coil, matrix Λ becomes zero and system (3.2.26) reduces to system (1.2.24), obtained by working since the beginning under this hypothesis.

3.3 The voltage characteristic

In the previous section we have seen that, in order to solve the equivalent electric and magnetic networks in the case where the coil is voltage driven, we must express the voltage across it as a function of the currents of the coil and the superconducting region and the fluxes of the magnetizable domain. In order to accomplish this task let us consider again the system of figure 3.2.1, which is also shown below for convenience.

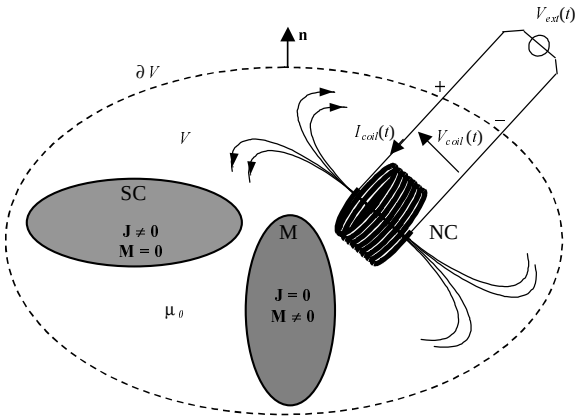

Figure 3.3.1: scheme of the considered system

When a current start to circulate in the coil some shielding currents and magnetization are induced in the superconducting and the magnetizable domain respectively, therefore some energy is passed to the system and stored in the magnetic form. Part of this energy can also be irreversibly transformed in heat due to Joule effect or hysteresis. However such an energy transfer is accompanied by the rise of some voltage across the terminals of the coil. Let us see this more in detail and start to apply the Poynting theorem to the volume V, enclosed by the outward oriented surface ∂V shown in the figure, thus to obtain

$$0 = \int_V \mathbf{H}(\mathbf{x},t)\cdot\frac{\partial \mathbf{B}(\mathbf{x},t)}{\partial t}\,d^3\mathbf{x} + \int_V \mathbf{E}(\mathbf{x},t)\cdot\frac{\partial \mathbf{D}(\mathbf{x},t)}{\partial t}\,d^3\mathbf{x} + \int_V \mathbf{E}(\mathbf{x},t)\cdot\mathbf{J}(\mathbf{x},t)\,d^3\mathbf{x} + \oint_{\partial V}\mathbf{E}(\mathbf{x},t)\times\mathbf{H}(\mathbf{x},t)\cdot\mathbf{n}\;d^2\mathbf{x} \tag{3.3.1}$$

The second integral on the right side does not contributes, since for the considered system the magnetoquasistatics approximation holds and the displacement current can be neglected everywhere. By expressing the magnetic flux density **B** as the curl of the magnetic vector potential **A** it is possible to rewrite the first integral on the right side of equation (3.3.1) as follows

$$\int_V \mathbf{H}(\mathbf{x},t)\cdot\frac{\partial \mathbf{B}(\mathbf{x},t)}{\partial t}\,d^3\mathbf{x} = \oint_{\partial V}\left(\frac{\partial \mathbf{A}(\mathbf{x},t)}{\partial t}\times\mathbf{H}(\mathbf{x},t)\right)\cdot\mathbf{n}\;d^2\mathbf{x} + \int_V\left(\frac{\partial \mathbf{A}(\mathbf{x},t)}{\partial t}\cdot\mathbf{J}(\mathbf{x},t)\right)d^3\mathbf{x} \tag{3.3.2}$$

By substituting equation (3.3.2) in equation (3.3.1) it follows

$$0 = \int_V\left(\frac{\partial \mathbf{A}(\mathbf{x},t)}{\partial t}\cdot\mathbf{J}(\mathbf{x},t)\right)d^3\mathbf{x} + \int_V \mathbf{E}(\mathbf{x},t)\cdot\mathbf{J}(\mathbf{x},t)\,d^3\mathbf{x} + \oint_{\partial V}\left(\mathbf{E}(\mathbf{x},t)+\frac{\partial \mathbf{A}(\mathbf{x},t)}{\partial t}\right)\times\mathbf{H}(\mathbf{x},t)\cdot\mathbf{n}\;d^2\mathbf{x} \tag{3.3.3}$$

By expressing the field $\mathbf{E}+\frac{\partial \mathbf{A}}{\partial t}$ through the gradient of the scalar electric potential the last term of equation (3.3.3) can be given as

$$\oint_{\partial V}\left(\mathbf{E}(\mathbf{x},t)+\frac{\partial \mathbf{A}(\mathbf{x},t)}{\partial t}\right)\times\mathbf{H}(\mathbf{x},t)\cdot\mathbf{n}\;d^2\mathbf{x} = -\oint_{\partial V}\nabla\times\left(\varphi(\mathbf{x},t)\mathbf{H}(\mathbf{x},t)\right)\cdot\mathbf{n}\;d^2\mathbf{x} + \oint_{\partial V}\varphi(\mathbf{x},t)\nabla\times\mathbf{H}(\mathbf{x},t)\cdot\mathbf{n}\;d^2\mathbf{x} + \tag{3.3.4}$$

By substituting the Ampere law and equation (3.2.5) in equation (3.3.4) and considering that the first integral on the right side is zero for the integrand function has zero divergence at any point of V, it follows

$$\begin{aligned}&\oint_{\partial V}\left(\mathbf{E}(\mathbf{x},t)+\frac{\partial\mathbf{A}(\mathbf{x},t)}{\partial t}\right)\times\mathbf{H}(\mathbf{x},t)\cdot\mathbf{n}\;d^2\mathbf{x}=\\&=I_{coil}(t)\oint_{\partial V}\varphi(\mathbf{x},t)\mathbf{k}_{NC}(\mathbf{x})\cdot\mathbf{n}\;d^2\mathbf{x}=-I_{coil}(t)(\varphi_+(t)-\varphi_-(t))\end{aligned}\tag{3.3.5}$$

where it has been assumed that, at time t, the scalar potential is uniform and is equal to $\varphi_+(t)$ and $\varphi_-(t)$ over the small areas where the positive an the negative terminal of the coil intersect the surface ∂V respectively. By substituting equation (3.3.5) in equation (3.3.3) we obtain

$$I_{coil}(t)V_{coil}(t)=\int_V\left(\frac{\partial\mathbf{A}(\mathbf{x},t)}{\partial t}\cdot\mathbf{J}(\mathbf{x},t)\right)d^3\mathbf{x}+\int_V\mathbf{E}(\mathbf{x},t)\cdot\mathbf{J}(\mathbf{x},t)\,d^3\mathbf{x}\tag{3.3.6}$$

where $V_{coil}(t)$ represents the difference of the instantaneous potentials of the positive and the negative terminal, i.e. the voltage across the coil.

By splitting the volume integrals on the left side of equation (3.3.6) in the sum of the integrals over the volumes of the normal coil and the superconducting and the magnetizable regions (V_{NC}, V_{SC} and V_M respectively), we see that the latter does not contribute at all for the current density is zero all over V_M, therefore

$$\begin{aligned}I_{coil}(t)V_{coil}(t)=&\int_{V_{NC}}\left(\frac{\partial\mathbf{A}(\mathbf{x},t)}{\partial t}\cdot\mathbf{J}(\mathbf{x},t)\right)d^3\mathbf{x}+\int_{V_{NC}}\mathbf{E}(\mathbf{x},t)\cdot\mathbf{J}(\mathbf{x},t)\,d^3\mathbf{x}+\\&+\int_{V_{SC}}\left(\frac{\partial\mathbf{A}(\mathbf{x},t)}{\partial t}\cdot\mathbf{J}(\mathbf{x},t)\right)d^3\mathbf{x}+\int_{V_{SC}}\mathbf{E}(\mathbf{x},t)\cdot\mathbf{J}(\mathbf{x},t)\,d^3\mathbf{x}+\end{aligned}\tag{3.3.7}$$

Let us express the sum of the integrals over the SC volume as follows

$$\int_{V_{SC}} \left(\frac{\partial \mathbf{A}(\mathbf{x},t)}{\partial t} \cdot \mathbf{J}(\mathbf{x},t) \right) d^3\mathbf{x} + \int_{V_{SC}} \mathbf{E}(\mathbf{x},t) \cdot \mathbf{J}(\mathbf{x},t)\, d^3\mathbf{x} = - \oint_{\partial V_{SC}} \varphi(\mathbf{x},t) \mathbf{J}(\mathbf{x},t) \cdot \mathbf{n}\; d^2\mathbf{x} + \int_{V_{SC}} \varphi(\mathbf{x},t) \nabla \cdot \mathbf{J}(\mathbf{x},t)\, d^3\mathbf{x} \tag{3.3.8}$$

where ∂V_{SC} represents the border surface of V_{SC}. Both the integrals on the left side of equation (3.3.8) are zero; the first due to the fact that the current density has zero normal component at the interface ∂V_{SC} of the superconductor with the insulating media, and the second because of the solenoidality of **J**. This means that any thermal power produced inside the superconductor is accompanied by a decrease of the stored magnetic energy with an equal rate, no other sources participate to the balance. Therefore, by substituting equation (3.3.8) and the constitutive relation of the normal conducting material (the Ohm law) inside equation (3.3.7), it follows

$$V_{coil}(t) = \int_{V_{NC}} \left(\frac{\partial \mathbf{A}(\mathbf{x},t)}{\partial t} \cdot \mathbf{k}_{NC}(\mathbf{x}) \right) d^3\mathbf{x} + I_{coil}(t) \int_{V_{NC}} \rho \left| \mathbf{k}_{NC}(\mathbf{x}) \right|^2 \; d^3\mathbf{x} \tag{3.3.9}$$

where ρ is the resistivity of the coil material. By substituting the expression (3.1.2) of the magnetic vector potential, equations (3.2.3), (3.2.4) and (3.2.5), and the constitutive relation (3.2.2) inside equation (3.3.9) we obtain

$$\begin{aligned} V_{coil}(t) = & \left(\frac{\mu_0}{4\pi} \int_{V_{NC}} \left(\int_{V_{NC}} \mathbf{k}_{NC}^T(\mathbf{x}) \frac{\mathbf{k}_{NC}(\mathbf{x}')}{|\mathbf{x}-\mathbf{x}'|}\, d^3\mathbf{x}' \right) d^3\mathbf{x} \right) \frac{d}{dt} I_{coil}(t) + \\ & + \left(\frac{\mu_0}{4\pi} \int_{V_{NC}} \left(\int_{V_{SC}} \mathbf{k}_{NC}^T(\mathbf{x}) \frac{[\mathbf{K}_J(\mathbf{x}')]}{|\mathbf{x}-\mathbf{x}'|}\, d^3\mathbf{x}' \right) d^3\mathbf{x} \right) \frac{d}{dt} \mathbf{I}(t) + \\ & + \frac{d}{dt} \left(\frac{\mu_0}{4\pi} \int_{V_{NC}} \left(\int_{V_M} \mathbf{k}_{NC}^T(\mathbf{x}) \frac{\mathcal{M}_B([\mathbf{K}_B(\mathbf{x}')] \boldsymbol{\Phi}(\tau), \tau \le t) \times (\mathbf{x}-\mathbf{x}')}{|\mathbf{x}-\mathbf{x}'|^3}\, d^3\mathbf{x}' \right) d^3\mathbf{x} \right) + \\ & + I_{coil}(t) \int_{V_{NC}} \rho \left| \mathbf{k}_{NC}(\mathbf{x}) \right|^2 \; d^3\mathbf{x} \end{aligned} \tag{3.3.10}$$

Equation (3.3.10) which can be finally rewritten as

$$V_{coil}(t) = L_{coil}\frac{d}{dt}I_{coil}(t) + \mathbf{L}_{SC}^{T}\frac{d}{dt}\mathbf{I}(t) + \frac{d}{dt}\left(\Lambda_{M}\left(\mathbf{\Phi}(\tau), \tau \le t\right)\right) + R_{coil}\, I_{coil}(t) \qquad (3.3.11)$$

where the coefficient L_{coil} is the auto inductance that the coil would have in the empty space, R_{coil} is the coil resistance, $\boldsymbol{L}_{SC}$ is a constant vector, with $N_{C|SC}$ components, which gives account of the contribution of currents of SC to the voltage and Λ_M is a scalar function of the fluxes of M region, which is linear in case of linear material. Equation (3.3.11) points out the dependence of the voltage across the coil on the unknown of the equivalent electric and magnetic networks.

3.4 Equivalent circuit of a magnetic shield type SFCL

Fault Current Limiters are regarded as key components for modern power systems [64]. Among all possible limiting devices, the superconducting ones offer ideal characteristics: negligible impedance in nominal conditions and passive, i.e. reliable, switch to high impedance state in case of fault. There exist two basic configurations for a superconducting device able to limit the fault current inside a circuit: the resistive [65] and the inductive [66] type. In the former case the current of the protected circuit passes directly through a superconducting element, which is designed in a way to keep the local current density below the critical value in normal operating condition. As the circuit current exceeds a quenching value, the superconducting element enters the dissipative (normal) state and a growing resistance appears in the circuit. In the inductive type the current of the protected circuit circulates through a normal coil coupled, via a ferromagnetic core, with a superconducting tube which shields, through the induced currents, the magnetic field. This configuration is also referred to as magnetic shield type SFCL. Also in this case the device is designed in a way to maintain the currents induced in SC tube below the critical value in normal operating condition. As the current exceeds a quenching value, the superconducting element enters the SC/N transition and the shielding effect reduces; as a consequence the magnetic field penetrates the core and an increasing reactance appears in the circuit. Even though very simple under the conceptual point of view, the SFCLs present several critical aspects when their actual design and manufacturing is concerned. First of all, in order to achieve acceptable cooling cost, only high temperature superconductors can be taken in consideration. Different materials, such as YBCO films, Bi2223 wires and Bi2212 bulk are available today, however, their brittle nature and the hot spot problems [14,67], make it necessary to adopt composite structures with a mechanical substrate and an electrical bypass. The optimal exploitation of the SC properties of such materials and their actual limiting ability depends very much on the device architecture.

A great number of studies, both theoretical and experimental, has been carried out in recent years, showing the feasibility of both the two basic concepts of SFCLs [66-73]. Nevertheless, all these studies were mainly focused on the device only; though a crucial point, the interaction of these devices with power networks is still little investigated.

Actually, in order to evaluate how a SFCL can enhance the performance of a power system, a model of the device needs to be introduced in power system simulators [74-78]. The more this model well reproduces the features of the limiting behavior, the more the technical and economical benefits are accurately estimated. By stating an appropriate mathematical formulation, and using an efficient numerical technique, it is possible to calculate, for a given operating condition, the time evolution of the field quantities inside the SFCL and to deduce on its base, the waveforms of some integral quantities, e.g. the voltage, which are of a greater practical interest. This is what we usually call a numerical model of the device. The voltage waveform can be measured and the accuracy of the numerical model can be tested on the base of the experimental data. However, the experimental conditions used for testing the model are quite simple and sometimes far from those to which the device is subject to when it operates inside a power system. In order to study the reciprocal influence of the SFCL and the power system we must either include the power system in the numerical model or export the numerical model of the device only in a simulation environment dedicated to power systems. The first approach is practically impossible to follow, for an accurate simulation of such an huge system would demand calculation times and computer requirements impossible to achieve. The second approach is more feasible but not trivial, because the integration, inside a simulation environment usually based on circuit theory, of a model based on a finite element formulation requires some attention; the easiest way to accomplish this task is to express the finite element problem in a circuit form.

The model of the equivalent electric and magnetic networks presented in the previous sections, can be used to determine the equivalent circuit of a magnetic shield type fault current limiter. The equivalent circuit can be easily exported in a simulation environment dedicated to power systems to evaluate the reciprocal interaction.

Let us refer to the to the experimental framework described by Ueda *et al.* in [79], where a magnetic shield type SFCL is considered. A scheme of the device is shown in figure 3.4.1; the dimensions are quoted in mm

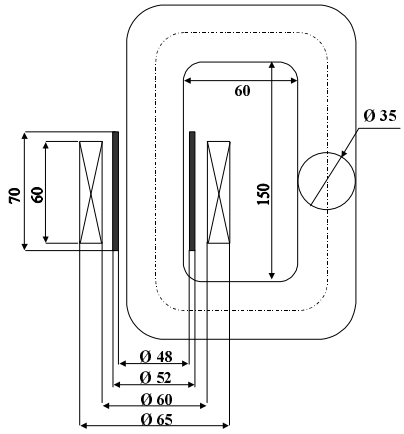

Figure 3.4.1: scheme of the magnetic shield type fault current limiter

The SC element is a Bi2223 tube [80], the copper coil is made of 4 layers of 55 turns each and the ferromagnetic core is a laminated closed magnetic loop. The whole device is immersed in a liquid nitrogen bath. The test circuit, which is shown in fig. 3.4.2, consists of a protective resistance R_{line} and a load resistance R_{load} series connected to the SFCL, and is supplied by a sinusoidal voltage generator. The circuit is controlled by a series connected switch SW1 and a secondary switch SW2, parallel connected to the load resistance, to command the fault event. A negligible shunt resistance, used for measuring the current, is also present. The values of the components of the test circuit are quoted in the figure. In the tests performed the control switch SW1 closes when the supply voltage crosses the zero; after three periods of the voltage waveform the switch SW2 closes and commands the fault and after a period both the switches open to allow recovering. Switch SW1 closes after a further period to verify the recovery. The expected nominal operation current has 10 A peaks while the non limited fault current has 80 A peak.

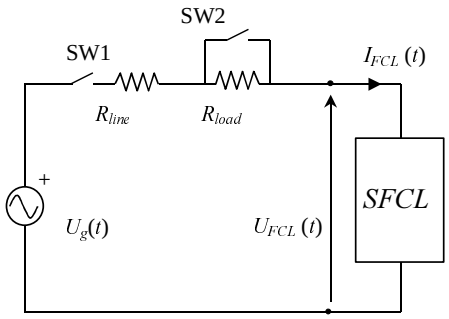

Frequency	*50 Hz*
$U_{g,\,max}$	*93 V*
R_{line}	*1.16 Ω*
R_{load}	*8.00 Ω*

Figure 3.4.2: test circuit

In order to define the equivalent circuit of the device, two meshes, one for the SC tube and one for the ferromagnetic core, are used. These meshes are shown in figure 3.4.3. Each mesh is made of triangular prisms; the axis of each prism is vertical for the SC tube while it is in the horizontal direction for the ferromagnetic core. The SC tube is divided into three rings with 24 triangular prisms each. The three rings are stacked on each other axially. For each ring, the prisms are arranged in 12 couples spanning all the ring thickness. This allows only one current per ring circulating in the azimuthal direction; no details of current distribution in the radial direction comes out from this discretization. The iron core mesh is made of one layer of 12 prisms. For the sake of simplicity an equivalent square cross section has been assumed instead of the actual circular one. Simulations with different number of elements either for the SC tube mesh as for the ferromagnetic core mesh have been considered in order to verify convergence of the numerical solution. The results corresponding to higher number of rings are the same as those obtained in the 3 rings case. The results corresponding to lower number of rings are significantly different.

To reproduce accurately the process of current penetration in the SC material a large number of elements is required for the SC mesh; however, when only the voltage across the normal conducting coil of the SFCL is considered, the difference in the numerical results arising from the details of current distribution, especially in the radial direction, is not significant. With reference to the SFCL voltage only, numerical convergence is reached even with coarse meshes of the SC tube, both in the radial and axial direction. Moreover, numerical simulations performed with packed meshes both in the radial and axial direction have shown that the radial and axial component of the

current density are negligible. Of course the equivalent circuit of the device refers to the smallest mesh which is able to reproduce the convergence value of voltage across the SFCL, with great advantages as long as simplicity of the equivalent circuit and CPU requirements are concerned.

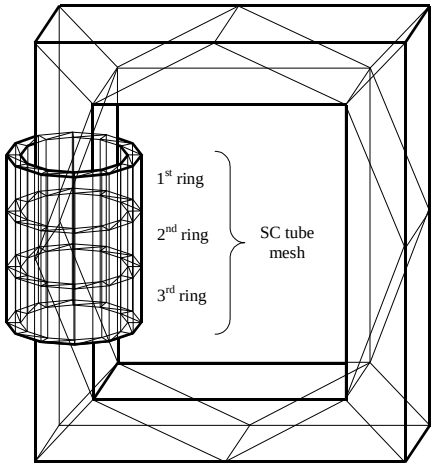

Figure 3.4.3: meshes of SC tube and ferromagnetic core

The equivalent circuit of the device obtained by the two meshes above under the assumption of linear magnetic core is shown in figure 3.4.4, together with the test circuit. This is a simple example of integration between a power system simulator (the scheme of the test circuit) and the numerical model of the device. The power law is assumed as constitutive relation of the superconductor. The thermal effects are not taken in account, i.e. the whole SC bulk is supposed to be in thermal equilibrium with the assigned temperature of 77 K and the critical current density used for power law refers to this temperature. The assumption of zero electric conductivity for the magnetic core is justified because of the lamination. Moreover, thanks to the linearity, the influence of the core on the current distribution inside the superconducting tube and on the voltage across the device, is directly incorporated in the auto/mutual induction coefficients as discussed in section 3.2 (see page 133-134), and the equivalent electric network does not need to be considered apart. The non linear resistors of any branch are indeed non linear passive controlled components, for they refer not only to current flowing on the branch, but also to currents of adjacent branches, as specified in section

3.2 (see page 131). The linear inductances represent both the self induction coefficient of the branch current and the mutual induction coefficients with all other currents. The values of the parameters used for deriving the equivalent circuit, i.e. the relative magnetic permeability of the linear core μ_r, the electrical resistivity ρ_{Cu} of the copper coil, the critical current density J_c of the SC tube and the exponent n of the *E-J* power law [79], are also quoted in figure 3.4.4.

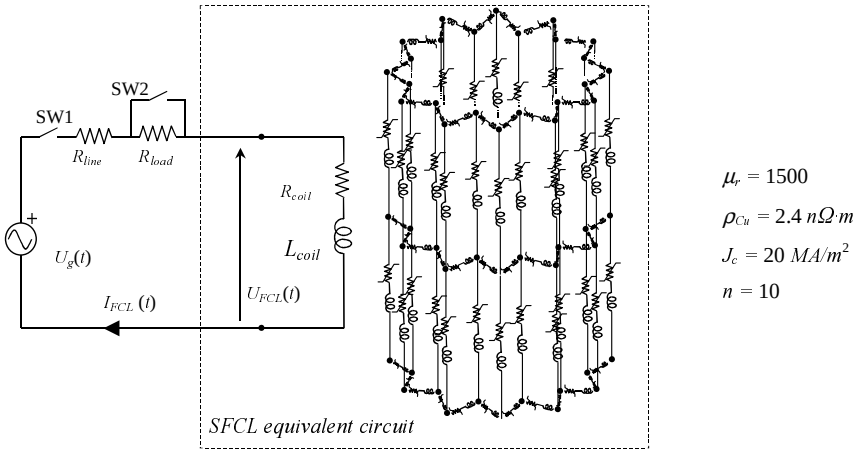

Figure 3.4.4: equivalent circuit of the magnetic shield type fault current limiter

The waveforms of the current and voltage across the device calculated by means of the equivalent circuit, labeled with "1 rings", are shown in figure 3.4.5 and 3.4.6 respectively, together with the experimental ones[1]. As it can be seen from the figures, a good agreement between experimental and calculated values is obtained, in particular during nominal conditions and during the first quarter of the period after the fault occurrence; the accurate simulation of the device dynamic during this time interval is crucial for the assessment of the SFCL impact on the power systems. In nominal conditions the effect of the shielding currents that circulate in the SC tube without losses is well reproduced, and the calculated value of the device impedance agrees very well with the experimental one. During the first quarter of the period after the fault starts, the shielding currents of the SC tube grow and begin producing significant losses

[1] The experimental results shown appear by courtesy of Dr. Hiroyuki Kado, Central Research Institute of Electric Power Industry, Yokosuka (Japan)

which are responsible of the limiting effect; the numerical calculated current of the device reaches a peak of 34.7 A, which is very near to the experimental one of 34.3 A. Some discrepancy is observed in the shape of the current and voltage waveform after the peak current is reached. The discrepancy can be due to thermal effect in the SC tube, the related saturation of the magnetic core, and the magnetic field dependence of the SC *E-J* characteristic, which are not considered in this paper. The numerical simulation show that, in nominal conditions, the contributions to the magnetic flux density in the ferromagnetic core induced by the coil and the SC tube almost cancels each other. When the current of the coil exceeds the value of the ratio of the SC tube critical current and the number of turns of the coil (about 13 A), the SC tube enters the superconducting transition and a net magnetic flux density begins to appear in the core for the contribution of the SC tube does not any more cancel the coil one. However, when the device current reaches its maximum value, the corresponding total magnetic flux density is equal to 0.9 T, thus leaving the core out of the saturation region. At the same instant, the average current density in the SC tube is more than twice the critical current density. Notwithstanding, core saturation certainly occurs if the reduction of the critical current density, due to the heating, impairs the contribution of the tube. Anyway, during the first quarter of period of the fault the power losses inside the SC tube probably do not produces a remarkable effect and the assumption of linearity for of the core can be utilized, thus allowing a simpler equivalent electric circuit of the device, without a significant loss of accuracy in the current-voltage characteristic. Figures 3.4.5 and 3.4.6 show also the numerical waveforms, labeled with “1 ring”, obtained by using for the SC tube a mesh having no axial subdivisions (the corresponding equivalent circuit has no axial branches and an unique, rather than three, loop made of azimuthal branches); as it can be seen a significant discrepancy is obtained with respect to the 3 (or more) ring case.

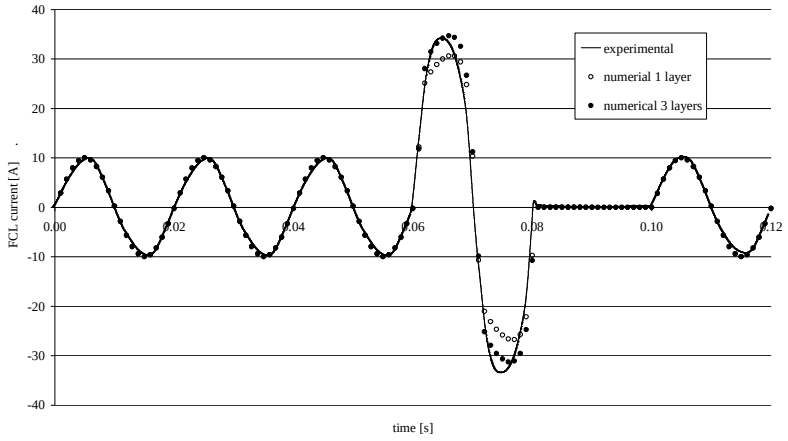

Figure 3.4.5: current of the SCFL

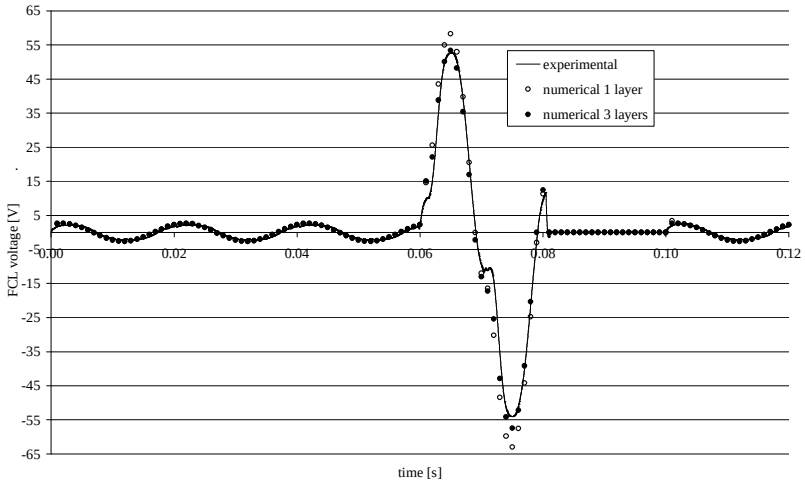

Figure 3.4.6: voltage of the SCFL

For what concerns the current distribution inside the SC tube, the numerical results show that no appreciable current flows in the axial direction. Therefore, the circuit branch connecting neighboring elements belonging to different rings can be eliminated from the equivalent circuit shown in figure 3.4.4, which reduces to the one shown in figure 3.4.7. Currents denoted by i_1, i_2, and i_3 are the azimuthal currents flowing in the three rings of the SC mesh. The non linear resistors $\mathcal{R}_1$, $\mathcal{R}_2$ and $\mathcal{R}_3$ are all defined by the law $U = K\left(i / i_c\right)^n sign(i)$, where i_c is the critical current of the SC ring corresponding

to the circuit loop (one third of the critical current of the whole SC tube), and *n* is the exponent of the power law assumed for modeling the SC material. The parameters of the SFCL equivalent circuit are reported in Table 3.4.I. The numerical results obtained by solving with a commercial circuit solver the reduced equivalent circuit agree with those obtained with the full equivalent circuit, shown in figures 3.4.5 and 3.4.6.

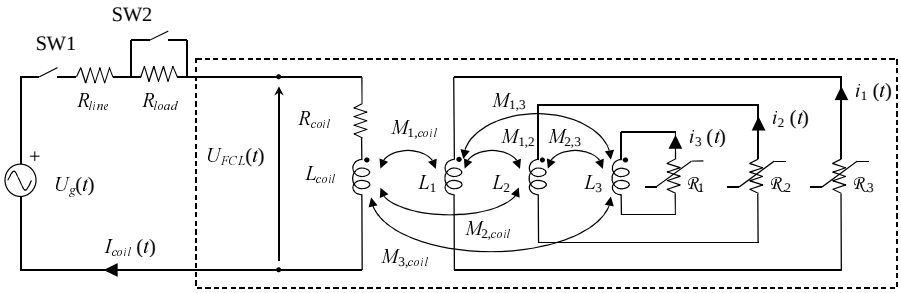

Figure 3.4.7: reduced equivalent circuit of the magnetic shield type fault current limiter

Table. 3.4.I: parameters of the reduced equivalent circuit

R_{coil}	0.136 Ω
L_{coil}	56.84 mH
$L_1 = L_3$	1.172 μH
L_2	1.169 μH
$M_{1,2} = M_{2,3}$	1.131 μH
$M_{1,3}$	1.121 μH
$M_{1,coil} = M_{3,coil}$	0.2528 mH
$M_{2,coil}$	0.2539 mH
K	21.96 μV
i_c	933 A
n	*10*

The reduced equivalent circuit obtained with the described procedure in the case of SC mesh made of one single ring coincides with the standard equivalent circuit reported in the literature [81-83], made of two coupled linear inductors, one of them connected to the protected circuit and the second series connected to a non-linear resistor, which gives account of the superconducting transition. However, as it can be seen from figures 3.4.5 and 3.4.6, for the considered device, the one-ring SC mesh, and

consequently the standard equivalent circuit, does not reproduces the experimental results as well as the three-ring based equivalent circuit does. Since the tube height is comparable with the coil height, the axial non uniformity of magnetic field produced by the coil leads to non uniform electromotive forces induced along the tube height. Consequently the azimuthal current cannot be assumed uniform and a multiple-rings SC mesh has to be used. In case of devices made of tubes which are “short” respect to the coil, the standard equivalent circuit can yield a good precision in numerical results.